
Article:
Pradal-Velázquez, E., Yang, F. and Sinclair, D.C. orcid.org/0000-0002-8031-7678 (2020) Synthesis and characterization of a pyrochlore solid solution in the Na2O-Bi2O3-TiO2 system. Journal of the American Ceramic Society. ISSN 0002-7820

https://doi.org/10.1111/jace.17380

Received: 27 May 2020 | Revised: 10 July 2020 | Accepted: 12 July 2020

DOI: 10.1111/jace.17380

Journal of the American Ceramic Society

ORIGINAL ARTICLE

Synthesis and characterization of a pyrochlore solid solution in the Na_2O-Bi_2O_3-TiO_2 system

Emilio Pradal-Velázquez | **Fan Yang** | **Derek C. Sinclair**

Department of Materials Science and Engineering, University of Sheffield, Sheffield, UK

Correspondence
Emilio Pradal-Velázquez, Departamento de Química Inorgánica y Nuclear, Facultad de Química, Universidad Nacional Autónoma de México, Ciudad de México, 04510, México.
Email: epradalv@quimica.unam.mx

Present address
Emilio Pradal-Velázquez, Departamento de Química Inorgánica y Nuclear, Facultad de Química, Universidad Nacional Autónoma de México, Ciudad de México, México
Fan Yang, Institute of Fuel Cells, School of Mechanical Engineering, Shanghai Jiao Tong University, Shanghai, P.R. China

Funding information
Science and Technology Facilities Council, Grant/Award Number: RB1720168; University of Sheffield; Consejo Nacional de Ciencia y Tecnología, Grant/Award Number: 327115

Abstract

The compositional limits of a previously reported (J. Am. Ceram. Soc., 61, 5-8. (1978)) but relatively unstudied sodium-bismuth titanate pyrochlore solid solution are revised and their electrical properties presented. The pyrochlore solid solution we report forms via a different mechanism to that originally reported and occurs in a different location within the Na_2O-Bi_2O_3-TiO_2 ternary system. In both cases, relatively large amounts of vacancies are required on the A-sites and on the oxygen sites, similar to that reported for undoped '$Bi_2Ti_2O_7$' pyrochlore. In contrast to '$Bi_2Ti_2O_7$', this ternary pyrochlore solid solution can be prepared and ceramics sintered using conventional solid-state methods; however, the processing requires several challenges to be overcome to obtain dense ceramics. This cubic pyrochlore series has low electrical conductivity (and does not exhibit any evidence of oxide-ion conduction) and exhibits relaxor ferroelectric behavior with a broad permittivity maximum of ~100 near room temperature. Variable temperature neutron diffraction data do not provide any conclusive evidence for a phase transition in the pyrochlore solid solution between ~4 and 873 K.

KEYWORDS

dielectric materials/properties, electroceramics, pyrochlore, relaxors

1 | INTRODUCTION

The Na_2O-Bi_2O_3-TiO_2 ternary system contains several phases with electrical functionalities. These include: (a) ferroelectric Aurivillius phases such as $Bi_4Ti_3O_{12}$, $Na_{0.5}Bi_{8.5}Ti_7O_{27}$, and $Na_{0.5}Bi_{4.5}Ti_4O_{15}$[1,2]; (b) ferroelectric perovskite $Na_{0.5}Bi_{0.5}TiO_3$ (NBT) that can exhibit high levels of oxide ion conduction[3] when prepared with deliberate Bi_2O_3 deficiency, ie, $Na_{0.5}Bi_{0.49}TiO_3$ or be an excellent dielectric or piezoelectric material if prepared nominally bismuth rich to compensate for Bi_2O_3 losses during processing, ie, $Na_{0.5}Bi_{0.51}TiO_3$; and (c) antiferroelectric $Bi_2Ti_4O_{11}$ that has been investigated as a microwave dielectric material.[4] In 1978 Uchida and Kikuchi reported on the phase equilibria at 1000°C for the TiO_2-rich end of the Na_2O-Bi_2O_3-TiO_2 ternary system. Their work included the first (and only, to the best of our knowledge) observation of a pyrochlore solid solution (Pss) with the composition x%Na_2O-25%Bi_2O_3-(75-x%) TiO_2 (x in mol %) with x ranging between 2.5% and 3.75% [5]; however, no electrical properties were reported.

The pyrochlore structure $A_2B_2X_6X'$ can be thought of as a defective fluorite (space group $Fd\bar{3}$ m) with ordered cation

and anion vacancies. The large A ions occupy distorted cubic sites, the B site has octahedral coordination, and the anions sit in 7/8 of the tetrahedral sites, the X site corresponds to the 48f Wycoff site and the X' site to the 8b site.[6] It is also often described as a rigid BX_6 octahedral network interpenetrated with a more flexible network of A_2X' chains. Pyrochlore oxides are known to exhibit diverse functionalities, including oxide ion conduction as electrolytes or mixed conductors,[7,8] enabled by the intrinsic anion vacancies and ease of migration through unoccupied octahedral sites. Undoped '$Bi_2Ti_2O_7$' is a pyrochlore that has been extensively studied due to its interesting optical and electrical properties; however, it cannot be prepared through conventional solid-state synthesis and sintering methods due to a narrow window of stability and incongruent melting of the material.[9,10] The $Bi_2Ti_2O_7$ pyrochlore has been studied through neutron diffraction by Radosavljevic et al[11] in 1998 at room temperature, by Hector and Wiggin[12] in 2004 at room temperature and 2 K, and by Kim et al[13] in 2009 at room temperature. They all conclude that $Bi_2Ti_2O_7$ is cubic (space group $Fd\bar{3}$ m) with a lattice constant between 10.36 and 10.38 Å. Radosavljevic et al conclude the material is bismuth and oxygen deficient (ie, $Bi_{1.74}Ti_2O_{6.62}$) as do Kim et al (ie, $Bi_{1.896}Ti_2O_{6.884}$). A review by Esquivel-Elizondo et al (Ref. 10) details and discusses several issues with this phase including the commonly observed bismuth deficiency of around 10%. The review also discusses how ferroelectric $Bi_4Ti_3O_{12}$ is a common impurity in the synthesis of '$Bi_2Ti_2O_7$' that can be difficult to detect using laboratory XRD, since characteristic diffraction peaks overlap with intense peaks associated with the pyrochlore phase. They note, however, that since $Bi_4Ti_3O_{12}$ and $Bi_2Ti_4O_{11}$ have an intense yellow color compared to the pyrochlore (which looks white as a phase-pure powder), the color can be a better way to detect these common impurities in small quantities rather than via XRD data. They also report a broad maximum in permittivity of ~115 at ~50°C between 500 and 2000 kHz in their microwave-assisted sintered pellets.

Known bismuth pyrochlores (ie, $Bi_2Zn_{2/3}Nb_{4/3}O_7$, $Bi_2Mg_{2/3}Nb_{4/3}O_7$, Bi_2ScNbO_7, Bi_2InNbO_7, and their analogous tantalates as well as $Bi_2Cu_{2/3}Nb_{4/3}O_7$ and $Bi_2Ni_{2/3}Nb_{4/3}O_7$) exhibit relaxor behavior and present broad permittivity maxima (between 67 and 250 at 1 MHz) with tanδ below 0.01. They also present clear dependence with frequency of the temperature at which the maxima occur and frequency dispersion of the real part of the permittivity below the maximum. Their permittivity maxima occur well below room temperature up to 1 MHz and it is in the microwave region where some of them have maxima approaching room temperature (eg, Bi_2InNbO_7 has a permittivity maximum around 284 K at 10 GHz).[14] Turner et al studied the dielectric properties of $Bi_2Ti_2O_7$ synthesized from titanium isopropoxide and bismuth nitrate (as described in Reference 10) and made into pellets using microwave-assisted sintering. They reported this pyrochlore, while exhibiting relaxor behavior, presents important and very noticeable differences in its electrical response when compared against other bismuth pyrochlores, mainly its permittivity at different frequencies does not converge at temperatures above the permittivity maximum and this maximum occurs at a higher temperatures (close to 300 K at 2 MHz compared against a maximum below 200 K for $Bi_2Zn_{2/3}Nb_{4/3}O_7$ at the same frequency).[15]

In our attempts to establish the composition-structure-property relationships of ternary phases within the Na_2O-Bi_2O_3-TiO_2 system, four different series of compositions were explored for the cubic pyrochlore Pss system and their compositions are given in Table S1. The first series (U) consisted of five compositions within the Pss range originally reported by Uchida and Kikuchi[5] which are represented by filled blue symbols in the phase diagram in Figure 1. This series was reported to exist around a fixed Bi_2O_3 (B) content of 25 mol% and variable Na_2O (N) and TiO_2 (T) mol% in the range 2.5%N and 72.5%T (U1) to 3.75%N and 71.25%T (U5). Although we obtained a pyrochlore as the main phase in all U series samples, significant amounts of the NBT perovskite were detected in all of them. Modified compositions corresponding to series A and B represented by filled black symbols in Figure 1 were explored to find a compositional range that yielded only the pyrochlore phase. The A and B series were constructed on fixed T content (71.8% and 71.25%, respectively) with variable N and B content in the range of 3.1%N and 25.1%B to 0.9%N and 27.3%B for series A and 2.45%N to 26.3%B to 0.85%N and 27.9%B for series B. The central sample for the U series (U3) with a T content of 71.8% was the starting location for the A-series, Figure 1. The B-series was based on the experimental findings that single-phase materials could be made at a lower fixed content of T. In addition, two further samples based on lower and higher T content than the A and B series were prepared with compositions of 1.24%N-27.9%B-70.82%T (Pss07) and 1.81%N-26.0%B-72.2%T (Pss10). These two samples were single phase based on laboratory XRD data and combining these with single-phase samples from the A and B series gives rise to our proposed Pss with general formula $Na_xBi_{1.9-4.6x}Ti_2O_{6.85-6.4x}$ with $0.07 \leq x \leq 0.10$. This is depicted as filled green symbols in Figure 1 and named Pss100x, ie, Pss07 to Pss10 with increasing Na_2O content. The locus of this solid solution clearly lies in a different region to the U series originally reported[5] with our Pss members having lower Na but higher Bi contents compared to the U series. We describe processing conditions suitable to obtain dense ceramics using conventional solid-state synthesis and report the electrical behavior observed across this revised solid solution and compare their behavior with existing Bi-based pyrochlore relaxor ferroelectrics.

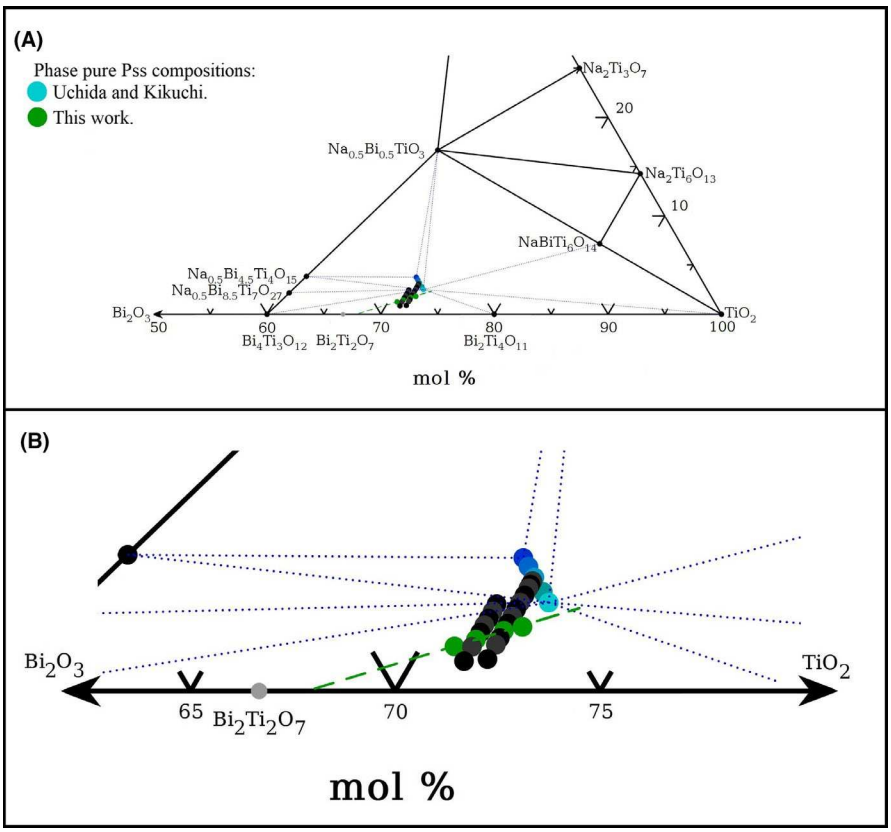

FIGURE 1 A, Partial Na_2O-Bi_2O_3-TiO_2 phase diagram indicating the phase equilibria studied by Uchida and Kikuchi at 1000°C with filled blue symbols representing the U series and the compositions found in this work to produce phase-pure samples (Pss series) at the same temperature shown by filled green symbols. B, Expanded section of the region in the ternary phase diagram showing the location of the compositions studied in this work and listed in Table S1. U series (blue filled symbols), A- and B-series (black filled symbols), and Pss series (filled green symbols)

2 | EXPERIMENTAL PROCEDURE

Dried Na_2CO_3 (99.5% Fisher), Bi_2O_3 (99.9% Acros Organics), and TiO_2 (99.9% Sigma Aldrich) were weighed in the stoichiometric amounts to prepare the compositions for series U, A, B, and Pss as listed in Table S1, then ball milled together in isopropanol for 6 hours. Powders for phase identification corresponding to series U were calcined once at 800°C for 2 hours and then at 1000°C for 2 hours in alumina crucibles; for series A, B, and Pss, a single calcination at 1000°C for 2 hours was used. Pellets were formed by uniaxial pressing and then submitted to 30 000 psi in a cold isostatic press to improve their density and sintered between 1100°C and 1200°C for 2 hours buried in sacrificial powder from the same batch (to minimize losses of Na_2O and Bi_2O_3) within alumina crucibles. Pellets for electrical measurements were prepared by a single step process taking green pellets of the mixed reactants buried in sacrificial powder and placed on top of "$Na_{0.5}Bi_{0.51}TiO_{3+\delta}$" ceramics before being sintered in air at 1200°C for 2 hours.

Phase identification was carried out on finely ground powders placed in plastic sample holders on a Bruker D2 Phaser diffractometer fitted with a Lynxeye detector and using Cu Kα radiation. Some data collected on small samples of crushed pellets were obtained with a STOE STADI-P diffractometer operating in transmission mode using Cu $K_{\alpha 1}$ radiation and a linear position sensitive detector. Neutron diffraction experiments were performed using the POLARIS diffractometer at ISIS between 4.2 and 873.17 K. Data from the detector banks 2 (25.99 °), 3 (52.21 °), 4 (92.59 °), and 5 (146.72 °) were used for analysis. Powders for the neutron diffraction experiments were loaded in vanadium cans, these were measured in a chamber which was evacuated to 10^{-5}-10^{-4} mbar before starting the measurements.

Rietveld refinements were performed using GSA[16] through EXPGUI[17] using space group $Fd\bar{3}$ m. The first refinement (for Pss07 at room temperature) was started from the structure published by Esquivel-Elizondo et al for $Bi_2Ti_2O_7$, refinements for other Pss compositions started from the results of the refinements of a composition with lower Na content and variable temperature refinements were started with the structure obtained for a previous temperature. The background of each histogram was initially fitted with a shifted Chebyschev polynomial using 12 terms (the number of terms was adjusted when necessary), once the backgrounds were fitted the lattice parameter was refined. Diffractometer constants (DIFC) for the lower resolution banks were refined using the room-temperature data while the constants for the backscattered bank were kept fixed, the DIFA coefficient accounting for the energy dependence of the neutron absorption by the sample was refined for all datasets. Peak profiles were refined next using function type 3 in GSAS, followed by the atomic positions (x,x,z) of the bismuth/sodium ions (constrained to be the same), and then by the atomic position

of the O1 ions (1/8,1/8,z) independently and, finally, both positions were refined together. Isotropic thermal displacement parameters ($U_{iso's}$) were refined starting with Bi/Na (again, constrained to have the same value) followed by O1 and O2 and, finally, all simultaneously. Next, both atomic positions and $U_{iso's}$ were refined together. The final step was the refinement of fractional site occupancies (F). The occupancies of O1, O3, and Ti did not vary significantly from the initial values and were kept fixed to those initial values, refining the sodium occupancy led to unstable refinements or unphysical results, hence, it was not refined but adjusted according to the nominal Na/Bi ratio.

A Perkin Elmer Pyris TGA was used for thermogravimetric analysis (TGA) using heating/cooling rates of 10 °Cmin^{-1} on ~70 mg of powder loaded on alumina pans.

Sintered ceramics for electrical characterization were polished and their faces painted at 800°C for 2 hours with gold paste (Heraus materials) to form the electrodes. Dielectric measurements were performed at 1, 10, 100, 250, and 1000 kHz using a Hewlett-Packard 4284A precision LCR meter. Impedance data were collected between 20 Hz and 1 MHz with an Agilent 4980A precision LCR meter. All the electrical characterization data were corrected for geometry before analysis. ZView (Scribner Associates) was used in the analysis of the impedance data. Extraction of bulk electrical properties was based on analysis of M'' spectroscopic plots. The height of a Debye peak in M'' (M''_{max}) corresponds to half the reciprocal of the capacitance (C) of the element responsible for it, ie, $C = 1/(2M''_{max})$. The angular frequency at which the peak appears (ω_{max}) is the reciprocal of the time constant (τ) for that element, since the time constant is the product of C and the resistance (R) of that element. The M'' peak position and height can be used to calculate R for that element, ie, $R = 2\ M''_{max}/\ \omega_{max}$. Bulk conductivity values (in units of S cm^{-1}) were obtained as 1/R, where R had been corrected for sample geometry.

3 | RESULTS

The five compositions prepared in series U ($Na_{2x}Bi_{4/3}Ti_{2-x}O_{6-x}$ with $1/15 < x < 1/10$) at 1000°C contained a pyrochlore as the main phase but also contained significant levels of the NBT perovskite as evidenced by the XRD patterns in Figure 2. Series A, B, and Pss were designed to find compositions where only the pyrochlore could be detected after processing powders at 1000°C in air. This required reducing the N content range of 2.5%–3.75% reported for Series U, Table S1. For series A and B, all samples with $N \geq 2.1\%$ (A1 to A7, B1, and B2) contained NBT in addition to a main phase pyrochlore. Those with $N \leq 1.5\%$ in series A (A10 to A12, B) and $N < 1.45\%$N (B7 and B8) contained $Bi_2Ti_4O_{11}$ and $Bi_4Ti_3O_{12}$ in addition to a main phase pyrochlore, see Figures S1 and S2. These compositions are represented by filled red/brown symbols in Figure 3 and the impurity phases are consistent with those predicted from the phase diagram at a higher/lower N content from that required for the pyrochlore solid solution. Several compositions with intermediate N-contents were single phase by laboratory XRD, ie, A7 to A9 and B3 to B6, Figures S1 and S2. Based on the recommendations made by Esquivel-Elizondo *et al* regarding the yellow color of common bismuth titanate impurities (eg,

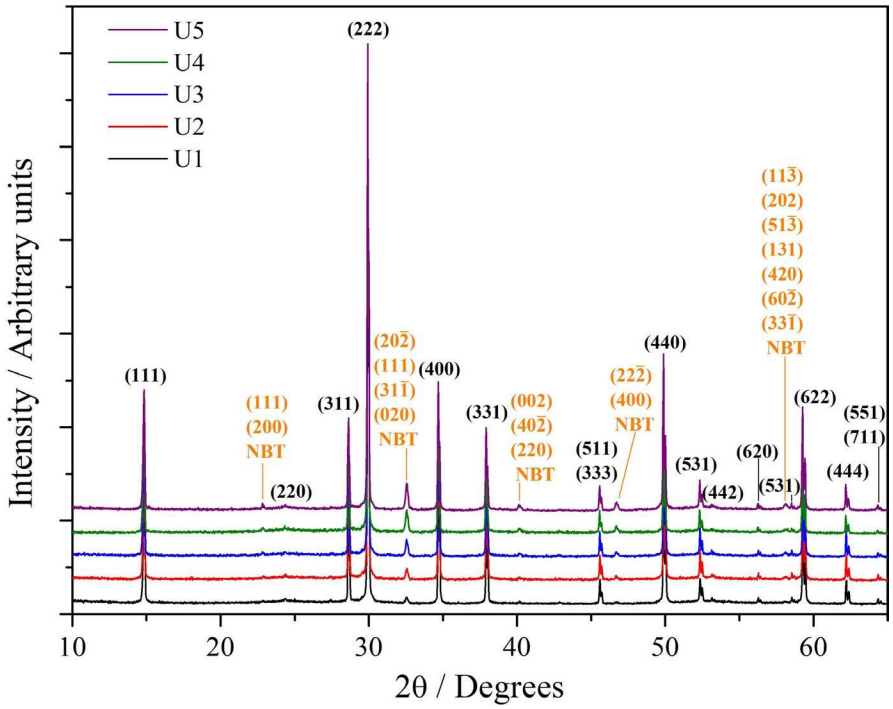

FIGURE 2 XRD patterns for 5 compositions in series U. Significant peaks arising from the NBT perovskite are marked with arrows

$Bi_4Ti_3O_{12}$), a single composition from each series (A9 and B6) with the least coloration was selected to determine the pyrochlore obtained follows an empirical formula $Na_xBi_{1.9-4.6x}Ti_2O_{6.85-6.4x}$ with $0.07 \leq x \leq 0.10$. Four samples were prepared with that formula (Pss07, Pss08, Pss09, and Pss10), which were single phase by laboratory XRD and are represented by filled green symbols in Figure 3. The remaining compositions for which only the pyrochlore were detected via XRD (A8, B3, B4, and B5) but had a more intense yellow coloration (therefore, presumed to contain impurity phases below the detection limit by XRD) is marked in filled yellow symbols in Figure 3.

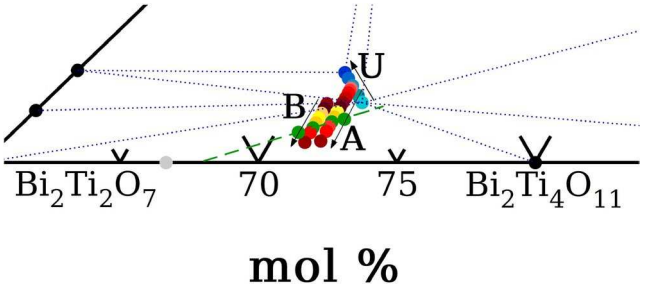

FIGURE 3 Details of the region in the ternary phase diagram for the compositions studied in this work as provided in Table S1. Filled blue symbols correspond to compositions within the Pss range reported in 5 but found to be phase mixtures in this study. Filled green symbols represent samples that were single phase by XRD which had the least coloration and, therefore, assumed to be single-phase Pss. Yellow filled symbols represent samples that were single phase by XRD but had intense yellow coloration and, therefore, assumed to contain low levels of impurities. Filled red/brown symbols represent samples for which impurities were readily detected via XRD

Sintering the Pss series to obtain single-phase dense ceramics was challenging. As exemplified with Pss09, treating calcined powders at 1050 or 1100°C results in the appearance of $Bi_2Ti_4O_{11}$ in the samples, Figure 4. This may be associated with loss of Na_2O and/or to the incongruent melting that also makes undoped '$Bi_2Ti_2O_7$' difficult to obtain. Using a single-step process in which the mixed reactants are pressed into pellets, buried in sacrificial powder, and then sintered avoids the formation of $Bi_2Ti_4O_{11}$ and produces phase-pure samples, Figure 4; however, pellet densities (estimated from the sample geometry) were significantly lower. For example, sintering Pss09 at 1100°C gave a density of 92% for a pellet of the calcined powder, whereas a density of ~75% was obtained for a single step pellet. Micrographs of a thermally etched (at 990°C) Pss09 single-step process pellet prepared at 1100°C are shown in Figure S3 to illustrate the homogeneity of the pellet and its porosity. Single-step process pellets sintered at 1200°C have densities of ~90%; however, EDX analysis revealed them to be contaminated with aluminum from the Al_2O_3 crucibles, Figure S4. In contrast, EDX analysis on low-density ceramics sintered at 1100°C does not detect any significant level of aluminum contamination, Figure S5. To obtain dense pellets without contamination from the Al_2O_3 crucibles, pellets were sintered on top of a previously sintered pellet of insulating NBT (nominally, $Na_{0.5}Bi_{0.51}TiO_{3\cdot 015}$) [3]. The compositions obtained from EDX spectra of two Pss09 pellets sintered at 1200°C (one made on top of an NBT pellet and one made only buried in sacrificial powder) are presented in Table S2. Values for Na and Bi are in good agreement with

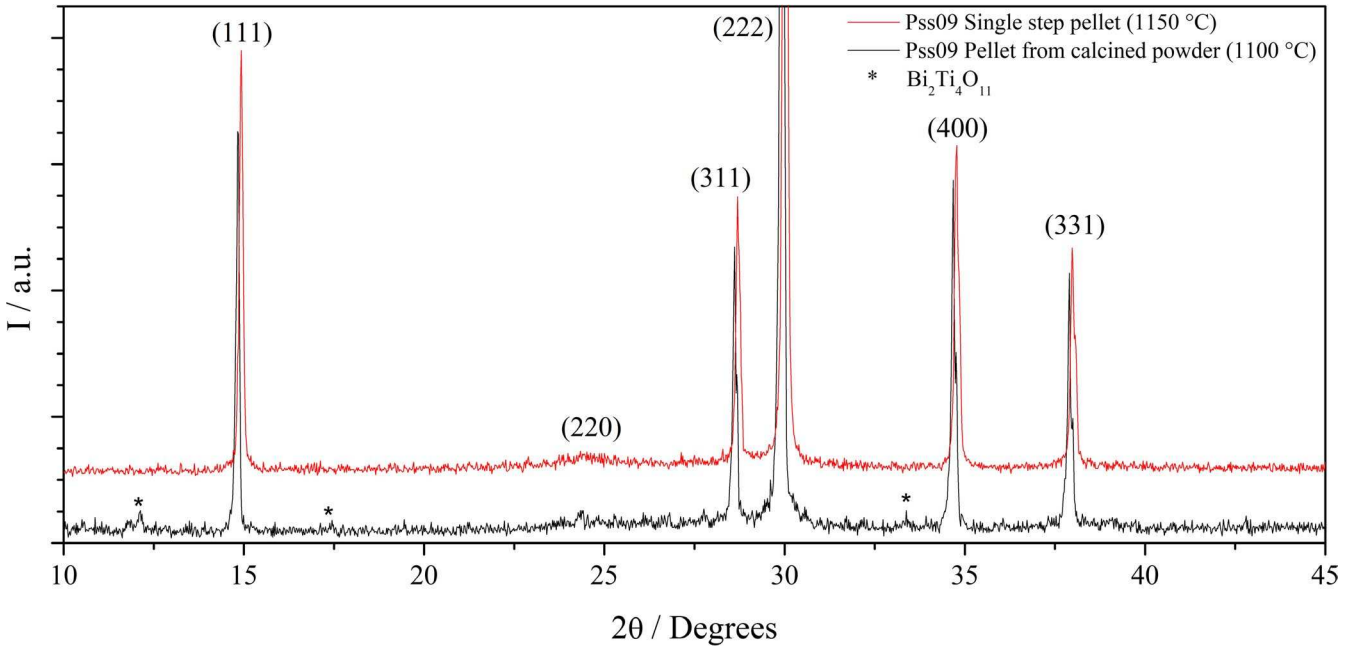

FIGURE 4 XRD patterns comparing Pss09 ceramics from a single-step process at 1150°C versus that from calcined powder sintered at 1100°C

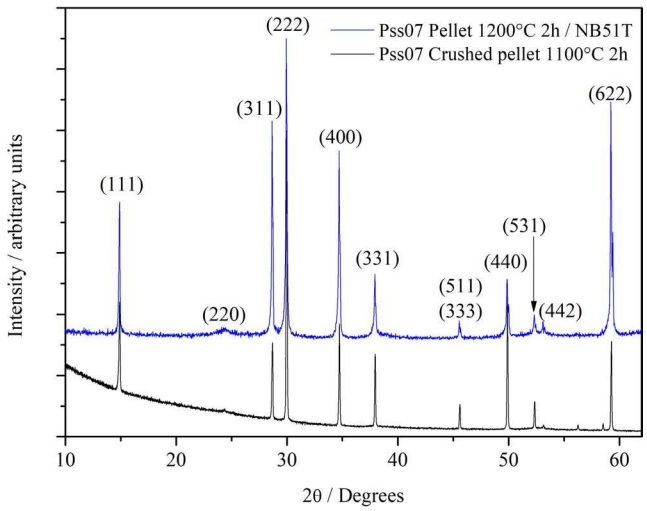

FIGURE 5 Secondary electron (top) and backscattered electron (bottom) micrographs of a thermally etched single-step process Pss09 ceramic sintered at 1100°C

the nominal composition and the titanium content seems to be slightly lower; however, it is important to note that the relative error for the small amount of sodium (a light element with low sensitivity in EDX) in the Pss is large, therefore, these quantifications should be used with caution. Figure 5 compares the XRD pattern for a Pss07 pellet prepared in this manner against a crushed pellet sintered at 1100°C (the data for this sample were collected on a STOE STADI-P diffractometer). It is noteworthy that the pellet sintered on top of an NB51T ceramic is textured as evidenced by the high relative intensities of the (311) and (622) peaks. Different processing routes to fabricate Pss ceramics are summarized in Table 1.

Powder neutron diffraction data[18] were collected at room temperature for crushed pellets (prepared from a single-step process at 1100°C on alumina crucibles with sacrificial powder) of Pss07 and Pss10 as well as calcined (at 1000°C) powders of Pss08 and Pss09. The diffraction patterns from this series shown in Figure 6 reveal small amounts of TiO_2 (marked with * on Figure 6) that had not been detected via laboratory XRD for all samples except Pss07 where the data could be fully indexed. Rietveld refinements of the data using space group $Fd\bar{3}m$ showed excellent agreement with a cubic pyrochlore structure. An example of a Rietveld refinement fitted plot is shown for Pss07 in Figure S6. The results obtained from the refinements are given in Tables S3 and S4, Figure 7 shows a linear trend for the change in lattice parameter across the Pss series. The bismuth and sodium ions are displaced from the high symmetry site to a higher multiplicity site (96g Wycoff site) where their coordination number is reduced; however, the displacement of the A-site ions does not seem to change significantly across the solid solution, Table S4. In all cases, the occupations of Ti and O1 sites (48f Wycoff site) did not vary significantly from 1 and were kept fixed at unity during the refinements. The O2 site (8b Wycoff site) was partially occupied in all 4 cases (ranging between 0.84 and 0.89) and there was also partial occupancy of the Na/Bi sites (between 0.79 and 0.83). The sodium content was adjusted based on the refined bismuth content according to the Na/Bi ratio in the nominal starting composition. This was required as attempts to simultaneously refine the sodium and bismuth contents and the amount of vacancies led to unstable refinements. Both Na_2O and Bi_2O_3 are volatile, so an assumption was made that the Na/Bi ratio would not change significantly between the nominal composition and the final product. This is supported by the EDX results in Table S2.

Variable temperature neutron diffraction experiments (4.2 to 300 K) were also performed for the Pss07 and Pss10. The samples were first cooled down to 4.2 K. No evidence of a

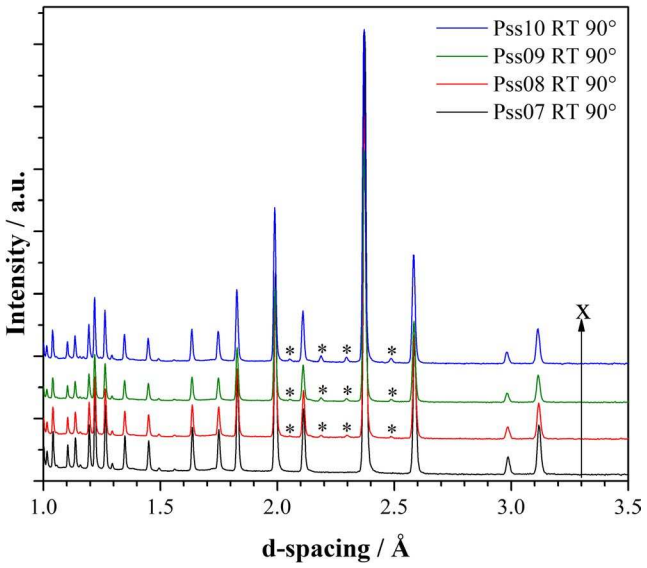

FIGURE 6 Neutron diffraction data for Pss collected at room temperature on the 90° detector. Peaks marked with * correspond to TiO_2

TABLE 1 Pss09 pellet processing summary

Processing	From calcined powder	Single step	Single step	Single step over NB51T pellet
Sintering temperature (°C)	1100	1100	1200	1200
Density (%)	92	75	89	95
Observations	$Bi_2Ti_4O_{11}$ detected via XRD	Phase pure	Phase pure but EDX shows Al contamination	Phase pure, no contamination

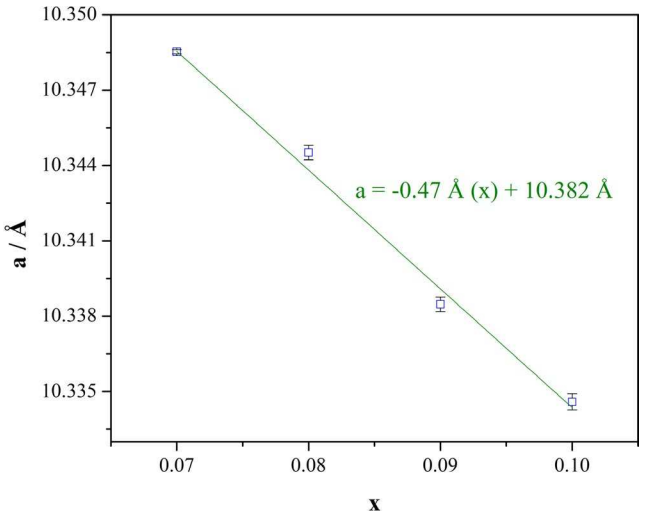

FIGURE 7 Change in room-temperature cell volume across the Pss

phase transition between 4.2 K and room temperature was observed as evidenced by the diffraction patterns in Figure S7 (a few additional peaks in the low-temperature data arise from the sample environment) and the near linear change of cell volume against temperature for Pss07, Figure S8.

Dielectric measurements were performed on pellets sintered at 1200°C on top of an NB51T pellet and 1 MHz data are presented in Figure 8A. The permittivity decreases with sodium content while the dielectric loss increases. The three compositions presented show good temperature stable permittivity between 85 and 125°C as well as low dielectric losses up to around 450°C. Subambient measurements were performed on a single-step Pss10 pellet prepared at 1100°C (relative density ~75%) which shows a clear shift in the maxima in permittivity and dielectric loss to higher temperatures with increasing frequency close to room temperature confirming relaxor behavior in these materials, Figure 8B. Typical impedance data for these samples are shown in Figure 9. A single response, which is attributable to the bulk based on its capacitance (of the order of 10 pF cm^{-1}), is observed as a semicircle in the complex impedance plot. M'' spectroscopic plots were used to extract the bulk conductivity for the Pss. The conductivity data are presented in Arrhenius format in

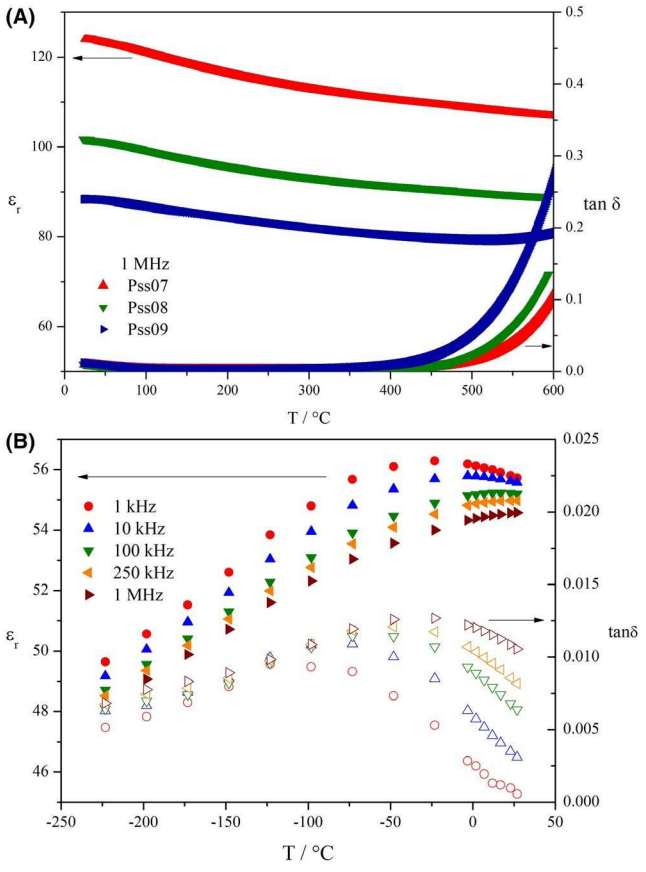

FIGURE 8 A, Temperature profiles of permittivity and dielectric loss for Pss ceramics (~ 95% relative density) at 1 MHz. B, Subambient temperature profiles of the permittivity and dielectric loss for Pss10 (~75% relative density)

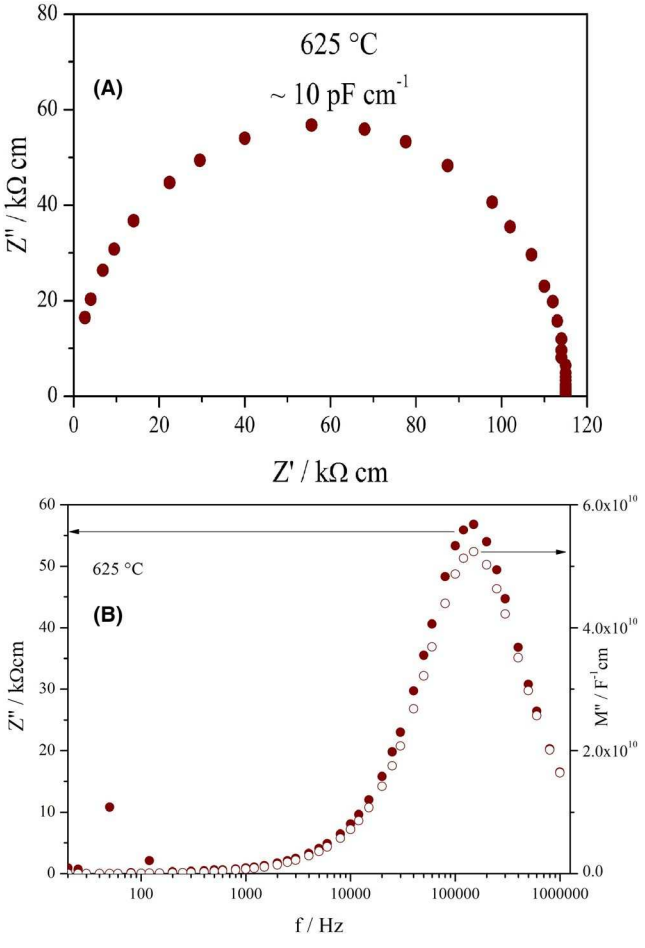

FIGURE 9 Typical impedance spectroscopy data collected for Pss07 at 625°C. (A) Complex impedance plot and (B) combined spectroscopic plots of the imaginary components of impedance and electric modulus

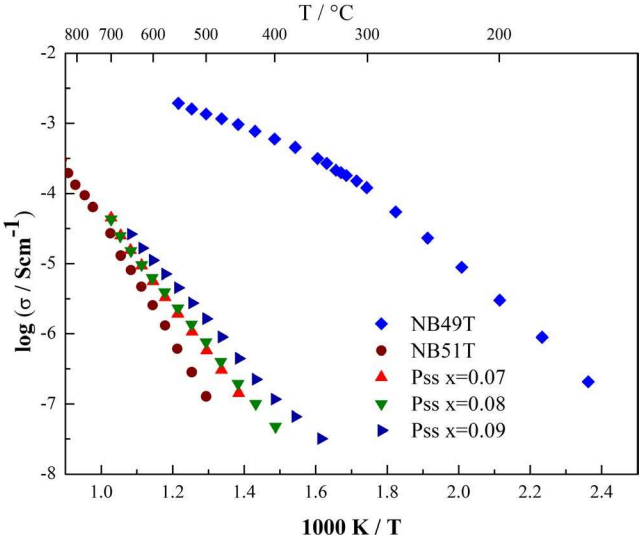

FIGURE 10 Arrhenius plots of bulk conductivity for the Pss series. Data for NB49T and NB51T from Reference 3 included for comparison

Figure 10. The bulk conductivities of the Pss are low and increases slightly with Na content, consistent with the trend observed for tan δ. The activation energy associated with the bulk conductivity was in the range ~1.1-1.4 eV.

4 | DISCUSSION

The XRD patterns in Figure 2 confirm the existence of a Pss but with different compositions from those originally reported,[5] as summarized in Figure 1. The originally reported Pss involved the "removal" of one Ti^{4+} for every two Na^+ ions introduced accompanied by the introduction of oxygen vacancies for charge balance. Since sodium ions are significantly larger than titanium (IV) ions, they most likely occupy the A-sites. It is unlikely that the doping mechanism involves the introduction of titanium vacancies and more oxygen vacancies while the A-site remains largely vacant (A-site nominal occupation in series U ranges from 75% to 81%). Since there is a relatively large amount of vacancies in the larger A-sites in this Pss, the introduced sodium ions could be accommodated in the structure. In our Pss several bismuth ions are substituted with each introduced sodium ion, which leads to a rapid increment of A-site and oxygen vacancies with sodium content. Piir et a[19] consider that '$Bi_2Ti_2O_7$' forms with A-site vacancies because the r_{Bi}/r_{Ti} ratio (1.17 Å/0.605 Å = 1.93[20]) is too large and falls outside the stability field for pyrochlores (1.48 to 1.80[7]). As shown in Figure 7, the lattice contracts with increasing Na_2O content, indicating the effective r_A/r_{Ti} ratio decreases with the introduction of Na^+ ions. Considering that Na^+ and Bi^{3+} ions have very similar radii (1.18 and 1.17 Å, respectively, for coordination number VIII[20]), the substitution of bismuth for sodium by itself would not change the effective A-site radius. The role of Na^+ ions in stabilizing the pyrochlore might be related to the more ionic character of the Na-O bonding compared against Bi^{3+} with its electron lone pair; however, the origin(s) of preferred distribution of A-site ions in the lattice remains an open question. Nevertheless, incorporation of Na ions is clearly beneficial in the stabilization of this pyrochlore phase given the ease with which these materials can be prepared by a conventional solid-state route in contrast to undoped '$Bi_2Ti_2O_7$' which requires alternative methods of synthesis.

An additional observation relevant to the stability of this Pss was the dramatic change in color of the powders on removal from the high-temperature ND experiments. The powders had been exposed to high vacuum at ~600°C and were black in appearance. Pre- and post-ND XRD data collected at room temperature on Pss07 showed the predominant phase to be a pyrochlore with only a slight shift of the peaks to lower angles and a small amount of secondary-phase TiO_2 becoming apparent post-ND, Figure S9. Figure S10 compares the ND data collected at 600°C and at RT for Pss07 and shows the appearance of TiO_2 but no other significant change besides the lattice expansion. Thermogravimetric analysis (TGA) on pre- and post-ND samples in air up to 700°C showed significant losses and gains in mass, respectively, indicating clear redox activity, Figure S11. The post-ND powders returned to an off-white appearance after the TGA experiment. The darkening of the powders under high vacuum at 600°C is attributed to reduction in some Ti^{4+} (d^0) to Ti^{3+} (d^1) ions, accompanied by a loss of oxygen. The recovery of the original color after heating in air at 700°C during the TGA experiment is linked to reoxidation of some Ti ions from Ti^{3+} (d^1) to $Ti4^+$ (d^0) ions, naturally accompanied by the reintroduction of oxide ions into the pyrochlore lattice. Given Ti^{3+} has a larger ionic radius compared to Ti^{4+}. The pyrochlore lattice expands as evidenced by the XRD peaks shifting to lower angles for the post-ND samples in Figure S9 (see inset). This expansion will reduce the r_{Bi}/r_{Ti} ratio and is more favorable for stabilization of the pyrochlore lattice. This observation, combined with the corresponding results, indicates that Ti-reduced Bi-based pyrochlores may have an enhanced field of stability compared to those based on fully oxidized Ti^{4+} ions from samples prepared in air. The pO_2 stability and redox activity of Pss requires further study, but is beyond the scope of this script.

Different processing conditions leading to different oxygen activities during synthesis could be the reason why our phase-pure Pss compositions do not match those reported by Uchida and Kikuchi.[5] An alternative explanation could be in the drying of reactants before batching. Particularly in the case of Na_2CO_3, which has the lightest molar mass and is the most hygroscopic among the reactants. Using "wet" Na_2CO_3 (ie, not drying prior to weighing) would result in the actual amount of Na_2O present in the batch being

significantly lower than the nominal amount.[21] According to our results where Na_2CO_3 was dried prior to use, the compositions reported by Uchida and Kikuchi have excess soda, which leads to the formation of the NBT perovskite as a secondary phase. The Rietveld refinements performed on the room-temperature ND data consistently show higher Bi and O content compared to the nominal starting compositions, Table S3. Na_2O loss during processing of the powders and ceramics is also a significant factor in the preparation of these materials based on the presence of TiO_2 as a secondary phase in ND data for most of the Pss samples and its appearance on Pss07 after the high-temperature ND experiment.

The pyrochlore solid solution may actually form over an area in the phase diagram. More series based on the compositions marked in green or yellow in Figure 3 with fixed N contents and variable B/T ratios could help clarify this and provide an insight into the unusual doping mechanism(s). The redox activity of these pyrochlores implies the ternary phase diagram used in Figures 1 and 3 may not be adequate to fully represent the compositional range for Pss and that a quaternary system would be a more complete representation. Further work is required to substantiate this suggestion but is beyond the scope of this script.

The Rietveld refinements on the ND data showed the oxygen vacancies associated with the A-site deficiency to be localized on the O2 sites (these sites also show particularly high thermal displacement parameters suggesting disorder in this sublattice, consistent with a random distribution of vacancies, Table S4). Oxygen vacancies on the O1 sites are considered to be essential for long-range oxygen migration in pyrochlores due to the site connectivity. [8,22] The lack of such vacancies in the Pss, therefore, explains the low electrical conductivity, Figure 10, despite the high oxygen vacancy concentration. The room-temperature ND data also confirm the formation of a solid solution, Figure 7, but the presence of TiO_2 as a secondary phase with increasing Na content means that a small adjustment to the compositional range we report is still required. The ND data collected at and below room temperature show no evidence of a phase transition that could be associated with the permittivity maxima observed around room temperature.

The broad permittivity maxima observed in Figure 8 are typical of bismuth-based pyrochlores and relaxors, however, the maxima appear at significantly higher temperatures than other bismuth pyrochlores. The frequency dependence for the position of these peaks illustrated in Figure 8B is also characteristic of relaxors. Figure S12 shows the linear relation between the logarithm of the frequency and the reciprocal temperature for the maxima in ε'' for Pss10, Figure 8B. The characteristic frequency of the relaxation (f_0) and activation energy (E_a) estimated from the linear fit (9.5×10^{12} Hz and 0.295 eV, respectively) are comparable with those of $Bi_{1.5}Zn_{0.92}Nb_{1.5}O_{6.92}$ (~10^{11} Hz and 0.2 eV [23]), which Turner et al consider representative of the relaxor behavior in Bi-based pyrochlores and compared to undoped "$Bi_2Ti_2O_7$".[15] Unlike undoped "$Bi_2Ti_2O_7$", the dielectric relaxation in the Pss exhibits a frequency similar to that of $Bi_{1.5}Zn_{0.92}Nb_{1.5}O_{6.92}$. As shown in Table S4, the A-site ions are displaced from the ideal site (presumably due to the lone electron pair on the bismuth ions), which allows the formation of polar nanoregions that give rise to the relaxor behavior. The most noticeable structural difference between this Pss and other bismuth pyrochlores is the large concentration of A-site and oxygen vacancies. The local interactions between these defects and the polar nanoregions responsible for the relaxor behavior could be the reason for the noticeably higher temperatures of the permittivity maxima. The electrical conductivity of the Pss is low, comparable to that of insulating NBT. Rietveld refinements on neutron diffraction data suggest that this is due to a lack of oxygen vacancies in the octahedral TiO_6 network, which are normally a prerequisite to allow long-range propagation of vacancies and, therefore, oxide-ion conductivity.

5 | CONCLUSIONS

A nonstoichiometric (A- and O-deficient) pyrochlore solid solution (Pss) is formed in the Na_2O-Bi_2O_3-TiO_2 system but at different compositions to that reported by Uchida and Kikuchi[5]; however, based on neutron diffraction data, the compositional limits require further minor adjustments. In contrast to undoped bismuth titanate pyrochlore, the Pss can be synthesized and sintered via conventional solid-state methods, however, ceramic processing is challenging. Obtaining phase-pure and dense ceramics requires fabrication on a compatible substrate, eg, NBT perovskite, as opposed to using Al_2O_3 crucibles/plates which result in Al contamination of the Pss. The ceramics are electrically insulating and exhibit relaxor ferroelectric behavior with ε_r maxima close to room temperature.

ACKNOWLEDGMENTS

Experiments at the ISIS Neutron and Muon Source were supported by beam-time allocation RB1720168 from the Science and Technology Facilities Council. The authors would like to thank Dr Ron Smith for assistance with data collection on POLARIS. EPV would like to thank CONACYT for his scholarship under ''Becas CONACYT al extranjero (registro 327115)" and the University of Sheffield for financial support.

ORCID

Emilio Pradal-Velázquez https://orcid.org/0000-0002-8302-2453

Fan Yang https://orcid.org/0000-0002-6428-7755
Derek C. Sinclair https://orcid.org/0000-0002-8031-7678

REFERENCES

1. Jardiel T., Caballero A.C., Villegas M.. Aurivillius ceramics: $Bi_4Ti_3O_{12}$-based piezoelectrics. J Ceram Soc Jpn. 2008;116(4):511–8.
2. Yokoi A., Sugishita J.. Ferroelectric properties of mixed bismuth layer-structured $Na_{0.5}Bi_{8.5}Ti_7O_{27}$ ceramic and $Sr_xNa_{0.5-x/2}Bi_{8.5-x/2}Ti_7O_{27}$ solid solutions. J Alloys Compd. 2008;452(2):467–72.
3. Li M., Pietrowski M.J., De Souza R.A., Zhang H., Reaney I.M., Cook S.N., et al. A family of oxide ion conductors based on the ferroelectric perovskite $Na_{0.5}Bi_{0.5}TiO_3$. Nat Mater. 2014;13(1):31–5.
4. Kahlenberg V., Böhm H.. The structures of α and β $Bi_2Ti_4O_{11}$. Acta Crystallogr B. 1995;B51:11–8.
5. Uchida K., Kikuchi T.. Subsolidus phase equilibria in the system Na_2O-Bi_2O_3-TiO_2 at 100°C. J Am Ceram Soc. 1978;61(1–2):5–8.
6. Laurita G., Vielma J., Winter F., Berthelot R., Largeteau A., Pötgen R., et al. From $Ag_2Sb_2O_6$ to $Cd_2Sb_2O_7$: Investigations on an anion-deficient to ideal pyrochlore solid solution. J Solid State Chem. 2014;210(1):65–73.
7. Subramanian M., Aravamudan G., Subba R.G.. Oxide pyrochlores: a review. Prog Solid State Chem. 1983;15(2):55–143.
8. Wilde P.J., Catlow CRA. Defects and diffusion in pyrochlore structured oxides. Solid State Ionics. 1998;112(3–4):173–83.
9. Kargin Y.F., Ivicheva S.N., Volkov V.V.. Phase relations in the Bi_2O_3-TiO_2 System. Russ J Inorg Chem. 2015;60(5):691–7.
10. Esquivel-Elizondo J.R., Hinojosa B.B., Nino J.C.. $Bi_2Ti_2O_7$: It is not what you have read. Chem Mater. 2011;23(22):4965–74.
11. Radosavljevic I., Evans JSO, Sleight A.W.. Synthesis and structure of pyrochlore-type bismuth titanate. J Solid State Chem. 1998;136(1):63–6.
12. Hector A.L., Wiggin S.B.. Synthesis and structural study of stoichiometric $Bi_2Ti_2O_7$ pyrochlore. J Solid State Chem. 2004;177(1):139–45.
13. Kim S.S., Park M.H., Chung J.K., Kim W.J.. Structural study of a sol-gel derived pyrochlore $Bi_2Ti_2O_7$ using a Rietveld analysis method based on neutron scattering studies. J Appl Phys. 2009;105:061641.
14. Cann D.P., Randall C.A., Shrout T.R.. Investigation of the dielectric properties of bismuth pyrochlores. Solid State Commun. 1996;100(7):529–34.
15. Turner C.G., Esquivel-Elizondo J.R., Nino J.C.. Dielectric properties and relaxation of $Bi_2Ti_2O_7$. J Am Ceram Soc. 2014;97(6):1763–8.
16. Larson A.C., Von Dreele R.B.. General Structure Analysis System (GSAS). Los Alamos National Laboratory Report LAUR. 2000. p. 86–748
17. Toby B.H.. EXPGUI, a graphical user interface for GSAS. J Appl Crystallogr. 2001;34:210–3.
18. Sinclair D.C., Pradal-Velázquez E., Smith R.I., Yang F., Wu P.. Structural characterisation of a pyrochlore solid solution in the Na_2O Bi_2O_3 TiO2 system. STFC ISIS Neutron and Muon Source. 2017; https://doi.org/10.5286/ISIS.E.RB1720168
19. Piir I.V., Koroleva M.S., Ryabkov Y.I., Korolev D.A., Chezhina N.V., Semenov V.G., et al. Bismuth iron titanate pyrochlores: thermostability, structure and properties. J Solid State Chem. 2013;204:245–50.
20. Shannon R.D.. Revised effective ionic radii and systematic studies of interatomic distances in halides and chalcogenides. Acta Crystallogr. 1976;A 32:751–67.
21. Li M., Zhang H., Cook S.N., Li L., Kilner J.A., Reaney I.M., et al. Dramatic influence of A-Site nonstoichiometry on the electrical conductivity and conduction mechanisms in the perovskite oxide $Na_{0.5}Bi_{0.5}TiO_3$. Chem Mater. 2015;27(2):629–34.
22. Wuensch B.J., Eberman K.W., Heremans C., Ku E.M., Onnerud P., Yeo EME, et al. Connection between oxygen-ion conductivity of pyrochlore fuel-cell materials and structural change with composition and temperature. Solid State Ionics. 2000;129(1):111–33.
23. Kamba S., Porokhonskyy V., Pashkin A., Bovtun V., Petzelt J.. Anomalous broad dielectric relaxation in $Bi_{1.5}Zn_{1.0}Nb_{1.5}O_7$ pyrochlore. Phys Rev B. 2002;66(5):054106.

SUPPORTING INFORMATION

Additional supporting information may be found online in the Supporting Information section.

How to cite this article: Pradal-Velázquez E, Yang F, Sinclair DC. Synthesis and characterization of a pyrochlore solid solution in the Na_2O-Bi_2O_3-TiO_2 system. *J Am Ceram Soc*. 2020;00:1–10. https://doi.org/10.1111/jace.17380